Morphometry of widespread tidal meander cutoffs discloses similarity to fluvial morphodynamics

C. Gao[1,2], E.D. Lazarus[3], A. D'Alpaos[2], M. Ghinassi[2], A. Ielpi[4], G. Parker[5,6], A. Rinaldo[7,8], P. Gao[9], Y.P. Wang[1,10], D. Tognin[7], and A. Finotello[2,*]

[1] *Ministry of Education Key Laboratory for Coast and Island Development, School of Geographic and Oceanographic Sciences, Nanjing University, Nanjing, China.*

[2] *Dept. of Geosciences, University of Padova, Padova, Italy.*

[3] *School of Geography & Environmental Science, University of Southampton, Southampton, UK.*

[4] *Department of Earth, Environmental and Geographic Sciences, University of British Columbia-Okanagan, Kelowna, BC, Canada.*

[5] *Department of Civil & Environmental Engineering, University of Illinois, Urbana, IL, USA*

[6] *Department of Geology, University of Illinois, Urbana, IL, USA*

[7] *Department of Civil, Environmental, and Architectural Engineering, University of Padova, Padova, Italy*

[8] *Laboratory of Ecohydrology, Ecole Polytechnique Federale Lausanne, Lausanne, Switzerland*

[9] *Department of Geography and the Environment, Syracuse University, Syracuse, NY, USA.*

[10] *State Key Laboratory of Estuarine and Coastal Research, School of Marine Sciences, East China Normal University, Shanghai, China*

* Corresponding author: Alvise Finotello (alvise.finotello@unipd.it)

Key Points:

- Tidal meander cutoffs are far more common than typically thought and share remarkable morphometric similarities with fluvial counterparts.
- Similar mechanisms trigger cutoffs in both tidal and fluvial landscapes, with differences arising only during post-cutoff evolution.
- Tidal cutoffs seldom disconnect from parent channels and form oxbow lakes due to the enhanced hydrological connectivity of tidal wetlands.

Abstract

Similarities in planform dynamics between tidal and fluvial meandering channels contrast with the apparent lack in coastal wetlands of lateral-migration features like meander cutoffs and oxbow lakes, which led to the broad interpretation that tidal and fluvial meanders differ morphodynamically. We analyzed meander neck cutoffs from diverse tidal and fluvial environments worldwide, and show that tidal cutoffs are more widespread than believed. Their perceived paucity is a figment of coastal-wetland pronounced drainage density and hydrological connectivity, coupled with reduced size of most tidal channels and dense vegetation cover. Whereas these factors do not efface tidal meander cutoffs, they collectively inhibit oxbow-lake formation and render tidal cutoffs ephemeral, hardly detectable geomorphic features. We thus argue that similar morphodynamic processes drive cutoff formation in tidal and fluvial landscapes, with differences arising only during post-cutoff evolution. This bears important implications for understanding the ecomorphodynamics of coastal wetlands and predicting their long-term evolution.

Plain Language Summary

The sinuous channels that wander through tidal coastal wetlands look like meandering rivers. However, features of alluvial floodplains that indicate active river meandering over time, such as oxbow lakes and meander cutoffs, are difficult to find in tidal realms. Their apparent absence has led researchers to infer that tidal and river meanders differ in their evolutions. We re-examined this conclusion by identifying, measuring, and compiling examples of meander cutoffs from a variety of tidal coastal wetlands and fluvial floodplains worldwide. Our analysis suggests that the shapes and geometric properties of tidal and river cutoffs are indeed remarkably similar. This indicates that while tidal and fluvial environments differ in many ways, they nevertheless share the same physical mechanism affecting meander morphodynamical evolution. Differences do arise, however, after meanders have cut off. We observe that tidal meanders remain preferentially connected to the channel from which they originated, preventing the formation of crescent-shaped oxbow lakes and thus making tidal cutoffs more difficult to detect. Our results support a close similarity in meandering channel behavior across tidal and fluvial systems, thus opening new opportunities for how researchers model tidal wetlands numerically, with important implications for the effective conservation and restoration of these critical ecosystems.

1 Introduction

Sinuous meandering channels are common in fluvial and coastal landscapes (Leopold et al., 1964). Meandering channels migrate laterally through erosion and deposition of sediment along the outer and inner banks, respectively, of individual meander bends. As meanders evolve, channels frequently shortcut themselves through cutoffs and form oxbow lakes (hereinafter "oxbows"; Dunne & Aalto, 2013; Ielpi et al., 2023; Mason & Mohrig, 2019; Schwenk et al., 2015; Stølum, 1996). Cutoffs play a critical role in channel and floodplain evolution by reducing channel sinuosity, modifying rates of lateral migration, and affecting floodplain sedimentology, stratigraphy, and sediment residence times (Ielpi et al., 2021, 2023; Schwenk et al., 2015; Zinger et al., 2011). Oxbows are important not only from ecological perspectives (Dieras et al., 2013; Thomas et al., 2022) but also because they retain signatures of the flow characteristics that shaped them (Guo et al., 2019). Collectively, the dynamics of meander cutoffs, of which oxbows are one consequence, have broad implications for the flux, storage, and sequestration of terrestrial organic carbon (Torres et al., 2017; Walcker et al., 2021).

While meandering river floodplains feature visible evidence of meander migration such as scroll bars and cutoffs (Constantine & Dunne, 2008; Dunne & Aalto, 2013; Hooke, 2013; Ielpi et al., 2023), channels in tidal coastal floodplains have been thought to lack meander cutoffs and, therefore, morphological evidence of active meandering (Gabet, 1998; Johnson & Campbell, 1929) (Figure 1). The apparent tendency for sinuous tidal channels to be fixed in place – or at least the relative subtlety of their meandering dynamics – has been variously ascribed to ecomorphodynamics peculiar to coastal settings(Fagherazzi et al., 2004; Gabet, 1998; Garofalo, 1980; Hughes, 2012; Kleinhans et al., 2009; Solari et al., 2002). However, recent studies highlighted common morphodynamics in fluvial and tidal meanders, with similar planform dynamics, width-adjusted migration rates, and morphodynamic regimes in high-amplitude bends (Finotello et al., 2018, 2022; Gao, Finotello, & Wang, 2022; Shaari et al., 2020). This motivated us to question the perceived paucity of tidal meander cutoffs, and to further demonstrate the parallels between tidal and fluvial meandering channels. Here, we analyzed the planform geometry of N_t=600 tidal meander cutoffs identified in high-resolution satellite images from settings around the world, characterized by different tidal regimes, vegetation cover, and geomorphological backgrounds. Direct comparisons with cutoffs in meandering rivers (N_f=158) highlight geometric similarities that - with supporting evidence from theoretical, numerical, and field studies – are shared by morphodynamic processes in both tidal and fluvial realms.

2 Materials and Methods

2.1 Data collection

We used high-resolution satellite images, freely available from Google Earth Pro, to detect instances of meander cutoffs undisturbed by anthropic activities. The selected cutoffs encompass a wide variety of geographical locations, including coastal areas and inland alluvial plains, as well as a diversity of climatic and geological regions. Consequently, the sampled cutoffs reflect a range of hydrological and tidal regimes, sediment grain sizes, vegetation types, and land cover (Figure 1a-g). Our full dataset includes over 1200 examples of tidal cutoffs. Of these 1200 examples, 600 tidal cutoffs with clearly discernable boundaries were manually digitized as polygons using Google Earth Pro. The remainder lacked sufficient detail to be digitized due to poor preservation, dense vegetation canopy, low image resolution, complex morphology resulting from multiple cutoffs, or combinations of these factors, and were categorized as

"unanalyzed cases" (Gao & Finotello, 2023). Furthermore, we obtained an additional set of 158 fluvial cutoffs specifically digitized for comparative analyses. These cutoffs were extracted from rivers located in various regions, including the Amazon Basin, the conterminous USA and Alaska, Russia, Canada, Kazakhstan, and New Zealand. The selection was made to ensure a diverse range of channel sizes, with river widths spanning approximately four orders of magnitude (Figure 2).

Tidal cutoffs were also further classified based on tidal regime (microtidal n=315; mesotidal n=249; macrotidal n=36), vegetation cover (mangroves n=118; salt marshes n=433; tidal flats n=49), and geomorphological setting (bays n=164; back-barrier lagoons n=219; open coasts n=105; estuaries n=112) (Figure S1 in Supporting Information). The mean tidal range (MTR) for each study site was determined by analyzing tidal gauge data from Dong (2020) and the National Oceanic and Atmospheric Administration (https://tidesandcurrents.noaa.gov/), and individual study cases were classified as macro-tidal ($MTR > 4$ m), meso-tidal ($2 < MTR < 4$ m), and microtidal ($MTR < 2$ m).

We focus only on 'neck' cutoffs, formed when a high-amplitude loop gets isolated by the pinching connection of two adjacent bends. In the tidal settings we examined, we found no examples of 'chute' cutoffs, which are formed when a river bend is shortcutted by a new channel cutting through meander point bars.

2.2 Data analysis

To calculate their morphometric parameters, cutoff polygons were projected into appropriate UTM coordinates and converted to binary images. The channel centerline was computed based on a standard skeletonization procedure and then resampled using standard cubic spline-fit polylines. Cutoff endpoints were determined as the two branchpoints of the polygon skeleton (Figure 1l). To further characterize cutoff planform features, we computed the curvature $\mathcal{C}$ ([m^{-1}]) of the channel centerline as $\mathcal{C} = -d\theta/ds$, where θ is the angle between the tangent to the channel axis and an arbitrarily selected reference direction, $x(s)$ and $y(s)$ are the Cartesian coordinates of a given centerline point, and s is the intrinsic (i.e., along-channel) coordinate, assumed to be positive in the upstream (i.e., landward) direction. Because flow orientation within tidal meanders changes with tidal phases, we hereinafter assume a river-like reference system in which the terms 'upstream' and 'downstream' refer to landward and seaward directions, respectively.

After computing curvature, a Savitzky–Golay low-pass filter was applied to smooth noise in the original signal. Then, the apex of any individual cutoff was identified as the locus of maximum curvature (Figure 1l), and the cutoff asymmetry index was computed as $\mathcal{A} = (\ell_u - \ell_d)/(\ell_u + \ell_d)$ ([-]) where ℓ_u and ℓ_d are the distances between the cutoff apex and its upstream and downstream endpoints, respectively (Figure 1l). Negative values of $\mathcal{A}$ correspond to upstream-skewed cutoffs, and positive values of $\mathcal{A}$ to downstream-skewed cutoffs. Other morphometric parameters were also calculated, including: average channel width W ([-]);cutoff intrinsic length $\ell = \ell_u + \ell_d$ ([m]); cutoff cartesian length L ([m]), which is the planar distance between cutoff endpoints; cutoff sinuosity $\chi = \ell/L$ ([-]); cutoff amplitude A ([-]), computed as the maximum point-line distance between the cutoff centerline and the line connecting the two cutoff endpoints; cutoff radius of curvature R ([m]), defined as the radius of the best-fitting circle through all cutoff axis points; and flow-diversion angle Φ between the cutoff and its parent channel (Figure 1l). Because of bidirectional flow through tidal channels, morphodynamically meaningful flow-diversion angles can be identified at both the cutoff upstream (Φ_u) and

downstream (Φ_d) ends. By comparison, because of the unidirectional flow through river channels, only the upstream flow-diversion angle (Φ_u) is morphodynamically meaningful for fluvial cutoffs (Dieras et al., 2013).

To directly compare meander cutoffs of different sizes, dimensional morphometric variables were normalized using channel width (W), such that width-adjusted cutoff radius of curvature, amplitude, and lengths are defined as $R^* = R/W$, $A^* = A/W$, $L^* = L/W$, and $\ell^* = \ell/W$.

3 Results and Discussions

Dimensional morphometric features of individual cutoffs – R, A, and ℓ – all exhibit statistically significant (p-value < 0.01) power-law relationships to cutoff width W with matching best-fit power-law exponents and limited separation in power-law scaling constants (i.e., prefactors; Figure 2 and Figure S2 in Supporting Information). We also found a statistically significant quasi-linear relation between L and W (Figure S3 in Supporting Information), with $L \cong W$. The latter has been described previously as the condition leading to neck cutoff (Li et al., 2022), whereas L<W thus represents a geometrically impossible configuration (Hayden et al., 2021). Similarly, radius of curvature R=$W/2$ represents a physically meaningful lower bound, since the edges of a channel centerline with a radius of curvature smaller than half its width would intersect each other (Hayden et al., 2021). Although theoretically there are no physical limits to the development of both A and ℓ (besides the basic requirements that A>0 and ℓ>L in order for a centerline to be sinuous), meandering channel planforms in reality are fractal (Montgomery, 1996; Nikora, 1991). As a consequence, the prevalence of smaller curves weights the distribution of meander features toward the physically meaningful lower bound (Hayden et al., 2021; Vermeulen et al., 2016). Therefore, the observed scaling similarities might be due to the finite-width nature of the sinuous features we measured. Despite slight differences in the power-law scaling constants, the distributions reported in Figure 2 overlap substantially, making these dimensional metrics a relatively poor diagnostic with which to distinguish the fluvial or tidal nature of meander cutoffs (Figure S2 and Figure S3 in Supporting Information).

Characteristic differences do emerge, however, from the analyses of dimensionless cutoff morphometrics. Kolmogorov-Smirnov (KS) tests performed at standard 5% significance level highlight statistically significant differences between tidal and fluvial cutoffs for distributions of width-adjusted radius (R^*), amplitude (A^*), and intrinsic length (ℓ^*), along with the width-independent measures of sinuosity (χ), asymmetry ($\mathcal{A}$), and flow-diversion angles (Φ_u and Φ_d). Tidal cutoffs have smaller R^*, A^*, ℓ^*, and χ (Figure 3 and Table S1 in Supporting Information). Given that, before cutoff, each of these morphometric parameters is expected to increase with time, our findings could be broadly interpreted as showing a lower morphodynamic maturity in tidal cutoffs, thus pointing to a faster evolutionary trajectory. However, similar width-adjusted meander migration rates in tidal and fluvial settings (Finotello et al., 2018) contrast with such an interpretation. Furthermore, similar values of asymmetry ($\mathcal{A}$) and upstream flow-diversion angle (Φ_u) in tidal and fluvial cutoffs (Figure 3 and Table S1 in Supporting Information) not only reflects similar morphodynamic maturity but also suggests that similar mechanisms trigger cutoff formation, likely associated with the planform configuration of the parent channel (Dieras, 2013). Notably, both fluvial and tidal cutoffs exhibit negative median and peak values of the asymmetry index $\mathcal{A}$ (Figure 3e). That is, both types of cutoffs tend to be upstream-skewed, supporting similarity in their dominant morphodynamic regime (*sensu* Seminara et al., 2001).

We thus suggest that the smaller size and lower maturity of tidal relative to fluvial cutoffs depend on extrinsic factors broadly related to the hydro-ecogeomorphology of tidal wetlands

rather than on fundamental differences between tidal and fluvial meander morphodynamics. Specifically, we hypothesize that the high drainage density that typically characterizes tidal wetlands explains the comparably smaller size of tidal cutoffs, with enhanced hydrological connectivity justifying the apparent paucity of cutoff traces in tidal environments.

3.1 Drainage density control on meander cutoff formation

Meander migration in densely channeled tidal floodplains might shape the landscape differently than in fluvial contexts, where rivers can freely migrate laterally without intercepting other channels and confluences are comparatively infrequent. In contrast, the higher drainage density of tidal wetlands (*sensu* Marani et al., 2003) limits meander dynamics by preventing channels from freely migrating and meanders from fully developing without intercepting adjoining channels (Letzsch & Frey, 1980; Vilas et al., 1999). A similar dynamic is described in multi-thread, anastomosing rivers with individual meandering anabranches, where meander evolution is more likely to produce channel avulsions than meander cutoffs, due to enhanced drainage density compared to single-thread-meandering-river floodplains (Lagasse et al., 2004; Schumm et al., 1996). Accordingly, evidence from modern and ancient deposits shows that channel piracy (i.e., capture) in dense tidal networks (Figure S4 in Supporting Information) limits the lateral accretion of point bar bodies and can modify the network-scale distribution of the tidal prism, feeding back into the long term ecomorphodynamic evolution of the entire tidal system (Cosma et al., 2020; Finotello, Ghinassi, et al., 2020). Because tidal channel dynamics depends directly on the tidal prism (D'Alpaos et al., 2005; Finotello et al., 2018), which in turn responds to water surface gradients that generally decrease with decreasing distance among individual channels (Rinaldo et al., 1999), it follows that enhanced drainage density limits meander dynamics.

Our hypothesis is further corroborated by the evidence that distributions of R^*, A^*, L^*, and χ show only subtle variations across a range of tidal environments, with significant differences associated only with vegetation cover (Figure 3). Tidal cutoffs in salt marshes are smaller and less sinuous than those found in mangrove forests and tidal flats (Figure 3). This aligns with observations of tidal channel networks in salt marshes being more dense and hydrologically efficient (Kearney & Fagherazzi, 2016; Schwarz et al., 2022), and corroborates the idea that drainage density limits the development of tidal meandering cutoffs. Similar cutoff asymmetries ($\mathcal{A}$) and flow-diversion angles (Φ_u, Φ_d) among distinct tidal settings also suggests similarity in the morphodynamic processes responsible for cutoff development. Kolmogorov-Smirnov tests reveal significant differences in distributions of Φ_u, Φ_d, and $\mathcal{A}$ only based on geomorphological setting (Tables S2 to S13 in Supporting Information), but we find no differences in these morphometrics as a function of tidal range and vegetation cover despite the potential influence that both controls can exert on channel bank erosion (Gao, Finotello, D'Alpaos, et al., 2022; Gasparotto et al., 2022; Zhao et al., 2022).

3.2 Hydrological connectivity control on post-cutoff development

To further substantiate that differences in tidal and fluvial cutoff morphology stem from extrinsic factors and not intrinsic meander morphodynamics, we also examined the connection state of individual cutoffs with their parent channels. Once a river meander cutoffs, a plug bar forms in response to flow separation and reduced energetic conditions, leading to the gradual blockage of both cutoff entrance (Toonen et al., 2012). Eventually the cutoff becomes completely disconnected from the parent channel and forms an oxbow lake. Based on the presence and position of plug bars in our tidal and fluvial examples, we classified cutoffs into four groups:

237 completely connected, upstream connected, downstream connected, and disconnected (Figure 4).
238 The upstream- and downstream-connected cases can also be merged into a broader category of
239 partially connected cutoffs. Whereas more than 43% of fluvial cutoffs in our dataset are entirely
240 disconnected and only 28% are completely connected (Figure 4a), tidal cutoffs tend to remain
241 connected to their parent channels, with 87% of examples completely connected, 9% partially
242 connected, and only 4% entirely disconnected (Figure 4a).
243 This marked difference in the connection state of tidal versus fluvial cutoffs is not an apparent
244 function of tidal range, vegetation cover, and geomorphological setting (Figure 4). Moreover,
245 similar flow-diversion angles are observed in all our study cases, with median values consistently
246 ranging between 105° and 108° (Figure 4b,c) and further pointing to similar cutoff-triggering
247 mechanisms in fluvial and tidal landscapes. Morphological differences thus can be expected to
248 emerge once cutoffs have formed. Remarkably, the percentage of completely connected fluvial
249 cutoffs decreases as the flow-diversion angle increases, implying that larger Φ_u promote the
250 formation of plug bars and oxbows (Figure 4d). In contrast, tidal cutoffs tend to remain
251 connected to their parent channel irrespective of flow-diversion angles, whether upstream or
252 downstream (Figure 4d and Figure S5 in Supporting Information). Therefore, unlike fluvial
253 analogs, most tidal cutoffs remain hydrodynamically active to some extent, as they continue to
254 drain water from the adjoining tidal floodplains. Indeed, in stark contrast to meandering rivers,
255 the rate of lateral flow injections in tidal channels can greatly exceed the baseline flow rates,
256 resulting in a peculiar landward reduction of channel width (i.e., funneling; Lanzoni &
257 D'Alpaos, 2015). Notably, some tidal cutoffs may also remain connected to other active parts of
258 the network through minor lateral tributaries flowing directly into the cutoff (Figure 1a-I and
259 Figure S6 in Supporting Information). Hence, pronounced hydrological connectivity in tidal
260 wetlands prevents the formation of a plug bar and the subsequent evolution of tidal cutoffs into
261 oxbows. Such an evolutionary trajectory clearly differs from fluvial cutoffs, which are typically
262 abandoned and receive water and sediment input almost exclusively during major flood events
263 (Leopold et al., 1964; Shen et al., 2021) either through minor tie channels carved through the
264 plug bar (cf. Rowland et al., 2009) or as the entire alluvial plain floods (Shen et al., 2021).
265 Among the partially connected cutoffs in our dataset, the fluvial ones are preferentially
266 connected with their parent channels at the upstream end: plug bars tend to form at the cutoff
267 downstream end where flow separations and recirculation create a zone of dead velocity that
268 hinders mixing and promotes the deposition of fine sediment (Richards et al., 2018; Turnipseed
269 et al., 2021). In contrast, the few partially connected tidal cutoffs on record, tend to maintain
270 connectivity at the downstream end, aligned with the direction of ebb flows (Figure 4a). This
271 predominance can be attributed to the typically ebb-dominated character of tidal flows
272 (Fagherazzi et al., 2008; Finotello, Ghinassi, et al., 2020), which keeps the cutoff downstream
273 end periodically flushed.

274 *3.3 Meander cutoffs in tidal coastal landscapes: rare or everywhere?*

275 Abundant tidal cutoffs akin to oxbow-rich alluvial floodplains can be found in some tidal settings
276 with possibly lower drainage density and/or sediment supply that limits cutoff infill and
277 vegetation encroachment (Figure 1f-i and Figures S7 and S8 in Supporting Information). This
278 further corroborates the observation that tidal and fluvial meandering channels not only evolve
279 through similar morphodynamic processes, but also that tidal meanders are as prone to form
280 cutoffs as their fluvial counterparts given conducive environmental conditions. One thus
281 wonders, given the apparent ubiquity of cutoffs across a variety of tidal environments, why the

long-held notion prevailed that sinuous tidal channel bends are inherently unlikely to cut themselves off.

Our take is that, first, the characteristic width and amplitude of fluvial cutoffs may not vary significantly along a given reach of a meandering river between major tributaries, whereas meander cutoffs within a given tidal wetland can occur across a broad range of meander wavelengths and widths (Finotello, D'Alpaos, et al., 2020). Low-order, narrow tidal creeks are more frequently found than higher-order, wide channels and are thus the most likely to express cutoff development (Figure 1a-i and Figures S7 and S8 in Supporting Information). Yet small channels produce small cutoffs, which are especially challenging to observe from a broader spatial vantage particularly when the vegetation canopy is dense (e.g., in mangrove forests, Figure S9 in Supporting Information).

Another consideration is the sustained rate of vertical accretion that characterizes tidal wetlands, coupled with halophytic vegetation that can tolerate significant waterlogging stress. These factors may becloud cutoff traces (Figure 1b,d,f-I and Figure S9 in Supporting Information) through rapid sedimentation in the less hydrodynamically active portions of the cutoff, and the subsequent encroachment of vegetation. This levels out cutoff geomorphic expressions and further hinders their identification from aerial images. Although similar reasoning could apply to fluvial floodplains, reduced overbank sediment supply and slower rates of riparian vegetation growth in permanently waterlogged areas may prolong the time required to fill oxbows, making large river-cutoff scars identifiable from aerial photos for much longer periods (Figure 1j,k).

The apparent absence of tidal cutoffs is thus more an artifact of observations than a consequence of physical mechanisms. High drainage densities in tidal wetlands surely constrain the freely meandering of tidal channels (Figure S10 in Supporting Information). Yet the relatively small size of most tidal channels, along with the distinctive hydrological characteristics of tidal wetlands, contribute to the transient nature of tidal cutoffs and make them challenging to record. That is, unlike other features of meandering channels that might jump out at the observer, to find tidal cutoffs one has to go carefully looking for them.

The implied morphodynamic similarity between tidal and fluvial meanders is by no means diminished by the absence of prominent scroll bars in tidal wetlands, standing in stark contrast to river floodplains that often showcase intricate arrangements of sub-parallel scrolls indicative of previous channel locations (Figure 1k) (Dunne & Aalto, 2013; Strick et al., 2018). While there is no consensus on what drives the formation of scroll bars (van de Lageweg et al., 2014; Zen et al., 2017), we offer two possible, not mutually exclusive explanations for the absence of scroll bars in tidal meanders. One possibility is that tidal meanders undergo small incremental migrations during each tidal cycle, unlike fluvial meanders, which tend to migrate more episodically after the height of incrementally formed inner-bank levee-like features reaches a threshold condition (Mason & Mohrig, 2019; Wu et al., 2016). Another hypothesis is that sustained rates of vertical aggradation relative to lateral channel migration in tidal wetlands (cf. Brivio et al., 2016; Cosma et al., 2019) prevent scroll bars by systematically overshadowing any topographic irregularities. This explanation aligns with the lack of scroll bars in meandering streamflows evolving through curvature-driven fluvial-like mechanisms in aggradational settings such as coastal backwater areas (Swartz et al., 2020), peatlands(Candel et al., 2017; Guo et al., 2020), and submarine turbidity-current channels (Jobe et al., 2016; Morris et al., 2024)

4 Implications and Conclusions

Our findings demonstrate that meandering channels in tidal wetlands are as capable of forming meander cutoffs as their fluvial counterparts. From the morphometric evidence we have compiled, we suggest that the morphodynamic processes that drive tidal and fluvial cutoff development are fundamentally similar, with substantial differences arising only after cutoffs have formed. Rather than forming oxbows, tidal cutoffs remain preferentially connected to their parent channel owing to the pronounced hydrological connectivity that characterizes tidal wetlands. In this way, tidal meander cutoffs continue to drain (and help flood) the surrounding wetlands, remaining active and integral parts of the overall tidal channel network. Coupled with earlier theoretical, numerical, and field observations (Finotello et al., 2018, 2022; Gao, Finotello, & Wang, 2022), our results point to a complete morphodynamic analogy between tidal and fluvial meandering channels from meander inception to cutoff. Unified tidal and fluvial meander morphodynamics enable extending classical techniques employed for modeling meandering rivers numerically (Bogoni et al., 2017; Howard & Knutson, 1984; Parker et al., 2011; Seminara et al., 2001) to ecomorphodynamic models of tidal wetlands, where meandering is ubiquitous and yet routinely omitted in common practices. Such an advance in numerical modeling would have important implications for the conservation and restoration of critically endangered tidal wetlands, for example by helping improve assessments and estimations of past, present, and future blue carbon fluxes.

Acknowledgments

[Reviewers will be acknowledged]

This study is funded by the European Union – NextGenerationEU and by the University of Padua under the 2021 STARS Grants@Unipd programme "TiDyLLy- Tidal networks dynamics as drivers for ecomorphodynamics of low-lying coastal area" (to AF), as well as by a China Scholarship Council (CSC) scholarships (202106190084, to CG). AI is supported by a Discovery Grant from the Natural Sciences and Engineering Research Council of Canada.

Conflict of Interest Statement

The authors declare no conflict of interest.

Open Research

All the data presented and analyzed in this paper are freely available from a public Zenodo folder (Gao & Finotello, 2023)

References

Bogoni, M., Putti, M., & Lanzoni, S. (2017). Modeling meander morphodynamics over self-formed heterogeneous floodplains. *Water Resources Research*, *53*(6), 5137–5157. https://doi.org/10.1002/2017WR020726

Brivio, L., Ghinassi, M., D'Alpaos, A., Finotello, A., Fontana, A., Roner, M., & Howes, N. (2016). Aggradation and lateral migration shaping geometry of a tidal point bar: An example from salt marshes of the Northern Venice Lagoon (Italy). *Sedimentary Geology*, *343*, 141–155. https://doi.org/10.1016/j.sedgeo.2016.08.005

Candel, J. H. J., Makaske, B., Storms, J. E. A., & Wallinga, J. (2017). Oblique aggradation: a novel explanation for sinuosity of low-energy streams in peat-filled valley systems. *Earth Surface Processes and Landforms*, *42*(15), 2679–2696. https://doi.org/10.1002/esp.4100

Constantine, J. A., & Dunne, T. (2008). Meander cutoff and the controls on the production of oxbow lakes. *Geology*, *36*(1), 23–26. https://doi.org/10.1130/G24130A.1

Cosma, M., Ghinassi, M., D'Alpaos, A., Roner, M., Finotello, A., Tommasini, L., & Gatto, R. (2019). Point-bar brink and channel thalweg trajectories depicting interaction between vertical and lateral shifts of microtidal channels in the Venice Lagoon (Italy). *Geomorphology*, *342*, 37–50. https://doi.org/10.1016/j.geomorph.2019.06.009

Cosma, M., Finotello, A., Ielpi, A., Ventra, D., Oms, O., D'Alpaos, A., & Ghinassi, M. (2020). Piracy-controlled geometry of tide-dominated point bars: Combined evidence from ancient sedimentary successions and modern channel networks. *Geomorphology*, *370*, 107402. https://doi.org/10.1016/j.geomorph.2020.107402

D'Alpaos, A., Lanzoni, S., Marani, M., Fagherazzi, S., & Rinaldo, A. (2005). Tidal network ontogeny: Channel initiation and early development. *Journal of Geophysical Research: Earth Surface*, *110*(2), 1–14. https://doi.org/10.1029/2004JF000182

Dieras, P. L. (2013). The Persistence of Oxbow Lakes as Aquatic Habitats : an Assessment of Rates of Change and Patterns of Alluviation Doctorate of Philosophy, 177. Retrieved from http://orca.cf.ac.uk/49392/

Dieras, P. L., Constantine, J. A., Hales, T. C., Piégay, H., & Riquier, J. (2013). The role of oxbow lakes in the off-channel storage of bed material along the Ain River, France. *Geomorphology*, *188*, 110–119. https://doi.org/10.1016/j.geomorph.2012.12.024

Dunne, T., & Aalto, R. E. (2013). Large River Floodplains. In J. E. Schroder & E. Wohl (Eds.), *Treatise on Geomorphology* (Vol. 9, pp. 645–678). Elsevier. https://doi.org/10.1016/B978-0-12-374739-6.00258-X

Fagherazzi, S., Gabet, E. J., & Furbish, D. J. (2004). The effect of bidirectional flow on tidal channel planforms. *Earth Surface Processes and Landforms*, *29*(3), 295–309. https://doi.org/10.1002/esp.1016

Fagherazzi, S., Hannion, M., & D'Odorico, P. (2008). Geomorphic structure of tidal hydrodynamics in salt marsh creeks. *Water Resources Research*, *44*(2), 1–12. https://doi.org/10.1029/2007WR006289

Finotello, A., Lanzoni, S., Ghinassi, M., Marani, M., Rinaldo, A., & D'Alpaos, A. (2018). Field migration rates of tidal meanders recapitulate fluvial morphodynamics. *Proceedings of the National Academy of Sciences of the United States of America*, *115*(7), 1463–1468. https://doi.org/10.1073/pnas.1711330115

Finotello, A., D'Alpaos, A., Bogoni, M., Ghinassi, M., & Lanzoni, S. (2020). Remotely-sensed planform morphologies reveal fluvial and tidal nature of meandering channels. *Scientific Reports*, *10*(1), 1–13. https://doi.org/10.1038/s41598-019-56992-w

Finotello, A., Ghinassi, M., Carniello, L., Belluco, E., Pivato, M., Tommasini, L., & D'Alpaos, A. (2020). Three-Dimensional Flow Structures and Morphodynamic Evolution of Microtidal Meandering Channels. *Water Resources Research*, *56*(7), e2020WR027822. https://doi.org/10.1029/2020WR027822

Finotello, A., Capperucci, R. M., Bartholomä, A., D'Alpaos, A., & Ghinassi, M. (2022). Morpho-sedimentary evolution of a microtidal meandering channel driven by 130 years of natural and anthropogenic modifications of the Venice Lagoon (Italy). *Earth Surface Processes and Landforms*, *47*(10), 2580–2596. https://doi.org/10.1002/esp.5396

Gabet, E. J. (1998). Lateral Migration and Bank Erosion in a Saltmarsh Tidal Channel in San Francisco Bay, California. *Estuaries*, *21*(4), 745. https://doi.org/10.2307/1353278

Gao, C., & Finotello, A. (2023). Morphometry of widespread tidal meander cutoffs discloses

similarity to fluvial morphodynamics. [Dataset]. https://doi.org/10.5281/zenodo.8229300

Gao, C., Finotello, A., D'Alpaos, A., Ghinassi, M., Carniello, L., Pan, Y., et al. (2022). Hydrodynamics of Meander Bends in Intertidal Mudflats: A Field Study From the Macrotidal Yangkou Coast, China. *Water Resources Research*, *58*(12), 1–28. https://doi.org/10.1029/2022WR033234

Gao, C., Finotello, A., & Wang, Y. P. (2022). Predominant landward skewing of tidal meanders. *Earth Surface Processes and Landforms*, (July), 1–17. https://doi.org/10.1002/esp.5452

Garofalo, D. (1980). The Influence of Wetland Vegetation on Tidal Stream Channel Migration and Morphology. *Estuaries*, *3*(4), 258. https://doi.org/10.2307/1352081

Gasparotto, A., Darby, S. E., Leyland, J., & Carling, P. A. (2022). Water level fluctuations drive bank instability in a hypertidal estuary. *Earth Surface Dynamics*, *2080*(September), 1–28.

Guo, X., Chen, D., & Parker, G. (2019). Flow directionality of pristine meandering rivers is embedded in the skewing of high-amplitude bends and neck cutoffs. *Proceedings of the National Academy of Sciences of the United States of America*, *116*(47), 23448–23454. https://doi.org/10.1073/pnas.1910874116

Guo, X., Chen, D., Li, Z., Garcia, M. H., Parker, G., & Tanaka, G. (2020). Sinuous rivers in peat. In *River Flow 2020* (pp. 1575–1581). CRC Press. https://doi.org/10.1201/b22619-219

Hayden, A. T., Lamb, M. P., & Carney, A. J. (2021). Similar curvature-to-width ratios for channels and channel belts: Implications for paleo-hydraulics of fluvial ridges on Mars. *Geology*, *49*(7), 837–841. https://doi.org/10.1130/G48370.1

Hooke, J. M. (2013). River Meandering. In E. Wohl & Schroder (Eds.), *Treatise on Geomorphology* (Vol. 9, pp. 260–288). Washington: Elsevier. https://doi.org/10.1016/B978-0-12-374739-6.00241-4

Howard, A. D., & Knutson, T. R. (1984). Sufficient conditions for river meandering: A simulation approach. *Water Resources Research*, *20*(11), 1659–1667. https://doi.org/10.1029/WR020i011p01659

Hughes, Z. J. (2012). Tidal channels on tidal flats and marshes. In R. A. Davis & R. W. Dalrymple (Eds.), *Principles of Tidal Sedimentology* (Springer, pp. 269–300). Dordrecht: Springer. https://doi.org/10.1007/978-94-007-0123-6_11

Ielpi, A., Lapôtre, M. G. A., Finotello, A., & Ghinassi, M. (2021). Planform-asymmetry and backwater effects on river-cutoff kinematics and clustering. *Earth Surface Processes and Landforms*, *46*(2), 357–370. https://doi.org/10.1002/esp.5029

Ielpi, A., Viero, D. P., Lapôtre, M. G. A., Graham, A., Ghinassi, M., & Finotello, A. (2023). How Is Time Distributed in a River Meander Belt ? *Geophysical Research Letters*, *50*(2), e2022GL101285. https://doi.org/10.1029/2022GL101285

Jobe, Z. R., Howes, N. C., & Auchter, N. C. (2016). Comparing submarine and fluvial channel kinematics: Implications for stratigraphic architecture. *Geology*, *44*(11), 931–934. https://doi.org/10.1130/G38158.1

Johnson, D., & Campbell, M. R. (1929). Meanders in Tidal Streams: A Review and Discussion. *Geographical Review*, *19*(1), 135. https://doi.org/10.2307/208081

Kearney, W. S., & Fagherazzi, S. (2016). Salt marsh vegetation promotes efficient tidal channel networks. *Nature Communications*, *7*, 1–7. https://doi.org/10.1038/ncomms12287

Kleinhans, M. G., Schuurman, F., Bakx, W., & Markies, H. (2009). Meandering channel dynamics in highly cohesive sediment on an intertidal mud flat in the Westerschelde estuary, the Netherlands. *Geomorphology*, *105*(3–4), 261–276. https://doi.org/10.1016/j.geomorph.2008.10.005

Lagasse, P. F., Zevenbergen, L., Spitz, W., & Thorne, C. R. (2004). *A Methodology for Predicting Channel Migration NCHRP Project No. 24-16* (No. Ayres Associates) (Vol. 67). Fort Collins, CO. https://doi.org/10.1061/40581(2001)106

van de Lageweg, W. I., van Dijk, W. M., Baar, A. W., Rutten, J., & Kleinhans, M. G. (2014). Bank pull or bar push: What drives scroll-bar formation in meandering rivers? *Geology*, *42*(4), 319–322. https://doi.org/10.1130/G35192.1

Lanzoni, S., & D'Alpaos, A. (2015). On funneling of tidal channels. *Journal of Geophysical Research: Earth Surface*, *120*(3), 433–452. https://doi.org/10.1002/2014JF003203

Leopold, L. B., Wolman, M. G., & Miller, J. P. (1964). *Fluvial processes in geomorphology* (Freeman). San Francisco. Retrieved from http://catalogue.nla.gov.au/Record/2338901

Letzsch, W. S., & Frey, R. W. (1980). Deposition and erosion in a Holocene salt marsh, Sapelo Island, Georgia. *Journal of Sedimentary Petrology*, *50*(2), 529–542. https://doi.org/10.1306/212F7A45-2B24-11D7-8648000102C1865D

Li, Z., Gao, P., You, Y., Finotello, A., & Ielpi, A. (2022). Delayed neck cutoff in the meandering Black River of the Qinghai–Tibet plateau. *Earth Surface Processes and Landforms*, (September 2022), 1–12. https://doi.org/10.1002/esp.5534

Marani, M., Belluco, E., D'Alpaos, A., Defina, A., Lanzoni, S., & Rinaldo, A. (2003). On the drainage density of tidal networks. *Water Resources Research*, *39*(2), 1–11. https://doi.org/10.1029/2001WR001051

Mason, J., & Mohrig, D. (2019). Scroll bars are inner bank levees along meandering river bends. *Earth Surface Processes and Landforms*, *44*(13), 2649–2659. https://doi.org/10.1002/esp.4690

Montgomery, K. (1996). Sinuosity and fractal dimension of meandering rivers. *Area*, *28*(4), 491–500.

Morris, P. D., Sylvester, Z., Covault, J. A., Mohrig, D., & Dunlap, D. (2024). Fluvial-style migration controls autogenic aggradation in submarine channels: Joshua Channel, eastern Gulf of Mexico. In A. Finotello, Z. Sylvester, & P. R. Durkin (Eds.), *Meandering Streamflows: Patterns and Processes across Landscapes and Scales* (Vol. 540). Geological Society, London, Special Publications. https://doi.org/10.1144/SP540-2022-123

Nikora, V. (1991). Fractal structure of river planforms. *Water Resources Research*, *27*(6), 1327–1333.

Parker, G., Shimizu, Y., Wilkerson, G. V., Eke, E. C., Abad, J. D., Lauer, J. W., et al. (2011). A new framework for modeling the migration of meandering rivers. *Earth Surface Processes and Landforms*, *36*(1), 70–86. https://doi.org/10.1002/esp.2113

Richards, D., Konsoer, K., Turnipseed, C., & Willson, C. (2018). Characterising three-dimensional flow through neck cutoffs with complex planform geometry. *Fluvial Meanders and Their Sedimentary Products in the Rock Record*, *48*, 273–295. https://doi.org/10.1002/9781119424437.ch11

Rinaldo, A., Fagherazzi, S., Lanzoni, S., Marani, M., & Dietrich, W. E. (1999). Tidal networks 3. Landscape-forming discharges and studies in empirical geomorphic relationships. *Water Resources Research*, *35*(12), 3919–3929. https://doi.org/10.1029/1999WR900238

Rowland, J. C., Dietrich, W. E., Day, G., & Parker, G. (2009). Formation and maintenance of single-thread tie channels entering floodplain lakes: Observations from three diverse river systems. *Journal of Geophysical Research: Earth Surface*, *114*(2), 1–19. https://doi.org/10.1029/2008JF001073

Schumm, S. A., Erskine, W. D., & Tilleard, J. W. (1996). Morphology, hydrology, and evolution

of the anastomosing Ovens and King Rivers, Victoria, Australia. *Bulletin of the Geological Society of America*, *108*(10), 1212–1224. https://doi.org/10.1130/0016-7606(1996)108<1212:MHAEOT>2.3.CO;2

Schwarz, C., van Rees, F., Xie, D., Kleinhans, M. G., & van Maanen, B. (2022). Salt marshes create more extensive channel networks than mangroves. *Nature Communications*, *13*(1), 1–9. https://doi.org/10.1038/s41467-022-29654-1

Schwenk, J., Lanzoni, S., & Foufoula-Georgiou, E. (2015). The life of a meander bend: Connecting shape and dynamics via analysis of a numerical model. *Journal of Geophysical Research: Earth Surface*, *120*(4), 690–710. https://doi.org/10.1002/2014JF003252

Seminara, G., Zolezzi, G., Tubino, M., & Zardi, D. (2001). Downstream and upstream influence in river meandering. Part 2. Planimetric development. *Journal of Fluid Mechanics*, *438*, 213–230. https://doi.org/10.1017/S0022112001004281

Shaari, H., Mohd Nasir, Q., Pan, H. J., Mohamed, C. A. R., Yusoff, A. H., Wan Mohd Khalik, W. M. A., et al. (2020). Sedimentation and sediment geochemistry in a tropical mangrove channel meander, Sungai Kerteh, Peninsular Malaysia. *Progress in Earth and Planetary Science*, *7*(1). https://doi.org/10.1186/s40645-020-00362-y

Shen, Z., Aeschliman, M., & Conway, N. (2021). Paleodischarge reconstruction using oxbow lake sediments complicated by shifting hydrological connectivity. *Quaternary International*, *604*(July), 75–81. https://doi.org/10.1016/j.quaint.2021.07.004

Solari, L., Seminara, G., Lanzoni, S., Marani, M., & Rinaldo, A. (2002). Sand bars in tidal channels part 2. Tidal meanders. *Journal of Fluid Mechanics*, *451*(January), 203–238. https://doi.org/10.1017/s0022112001006565

Stølum, H. H. (1996). River meandering as a self-organization process. *Science*, *271*(5256), 1710–1713. https://doi.org/10.1126/science.271.5256.1710

Strick, R. J. P., Ashworth, P. J., Awcock, G., & Lewin, J. (2018). Geomorphology Morphology and spacing of river meander scrolls. *Geomorphology*, *310*(March). https://doi.org/10.1016/j.geomorph.2018.03.005

Swartz, J. M., Goudge, T. A., & Mohrig, D. C. (2020). Quantifying Coastal Fluvial Morphodynamics Over the Last 100 Years on the Lower Rio Grande, USA and Mexico. *Journal of Geophysical Research: Earth Surface*, *125*(6), 1–16. https://doi.org/10.1029/2019JF005443

Thomas, S. S., Constantine, J. A., Dethier, D., Thoman, J. W., Racela, J., Blau, E., & Landis, J. D. (2022). The importance of oxbow lakes in the floodplain storage of pollutants. *Geology*, *50*(4), 392–396. https://doi.org/10.1130/G49427.1

Toonen, W. H. J., Kleinhans, M. G., & Cohen, K. M. (2012). Sedimentary architecture of abandoned channel fills. *Earth Surface Processes and Landforms*, *37*(4), 459–472. https://doi.org/10.1002/esp.3189

Torres, M. A., Limaye, A. B., Ganti, V., Lamb, M. P., Joshua West, A., & Fischer, W. W. (2017). Model predictions of long-lived storage of organic carbon in river deposits. *Earth Surface Dynamics*, *5*(4), 711–730. https://doi.org/10.5194/esurf-5-711-2017

Turnipseed, C., Konsoer, K., Richards, D., & Willson, C. (2021). Numerical Modeling of Two-Dimensional Hydrodynamics in a Highly Curving and Actively Evolving Neck Cutoff Under Different Hydrologic Conditions. *Water Resources Research*, *57*(2), 1–14. https://doi.org/10.1029/2020WR027329

Vermeulen, B., Hoitink, A. J. F., Zolezzi, G., Abad, J. D., & Aalto, R. (2016). Multiscale structure of meanders. *Geophysical Research Letters*, *43*(7), 3288–3297.

https://doi.org/10.1002/2016GL068238

Vilas, F., Arche, A., Ferrero, M., & Isla, F. (1999). Subantarctic macrotidal flats, cheniers and beaches in San Sebastian Bay, Tierra Del Fuego, Argentina. *Marine Geology*, *160*(3–4), 301–326. https://doi.org/10.1016/S0025-3227(99)00021-3

Walcker, R., Corenblit, D., Julien, F., Martinez, J. M., & Steiger, J. (2021). Contribution of meandering rivers to natural carbon fluxes: Evidence from the Ucayali River, Peruvian Amazonia. *Science of the Total Environment*, *776*, 146056. https://doi.org/10.1016/j.scitotenv.2021.146056

Wu, C., Ullah, M. S., Lu, J., & Bhattacharya, J. P. (2016). Formation of point bars through rising and falling flood stages: Evidence from bar morphology, sediment transport and bed shear stress. *Sedimentology*, *63*(6), 1458–1473. https://doi.org/10.1111/sed.12269

Zen, S., Gurnell, A. M., Zolezzi, G., & Surian, N. (2017). Exploring the role of trees in the evolution of meander bends: The Tagliamento River, Italy. *Water Resources Research*, *53*(7), 5943–5962. https://doi.org/10.1002/2017WR020561

Zhao, K., Coco, G., Gong, Z., Darby, S. E., Lanzoni, S., Xu, F., et al. (2022). A Review on Bank Retreat: Mechanisms, Observations, and Modeling. *Reviews of Geophysics*, *60*(2), 1–51. https://doi.org/10.1029/2021rg000761

Zinger, J. A., Rhoads, B. L., & Best, J. L. (2011). Extreme sediment pulses generated by bend cutoffs along a large meandering river. *Nature Geoscience*, *4*(10), 675–678. https://doi.org/10.1038/ngeo1260

Figures and Tables

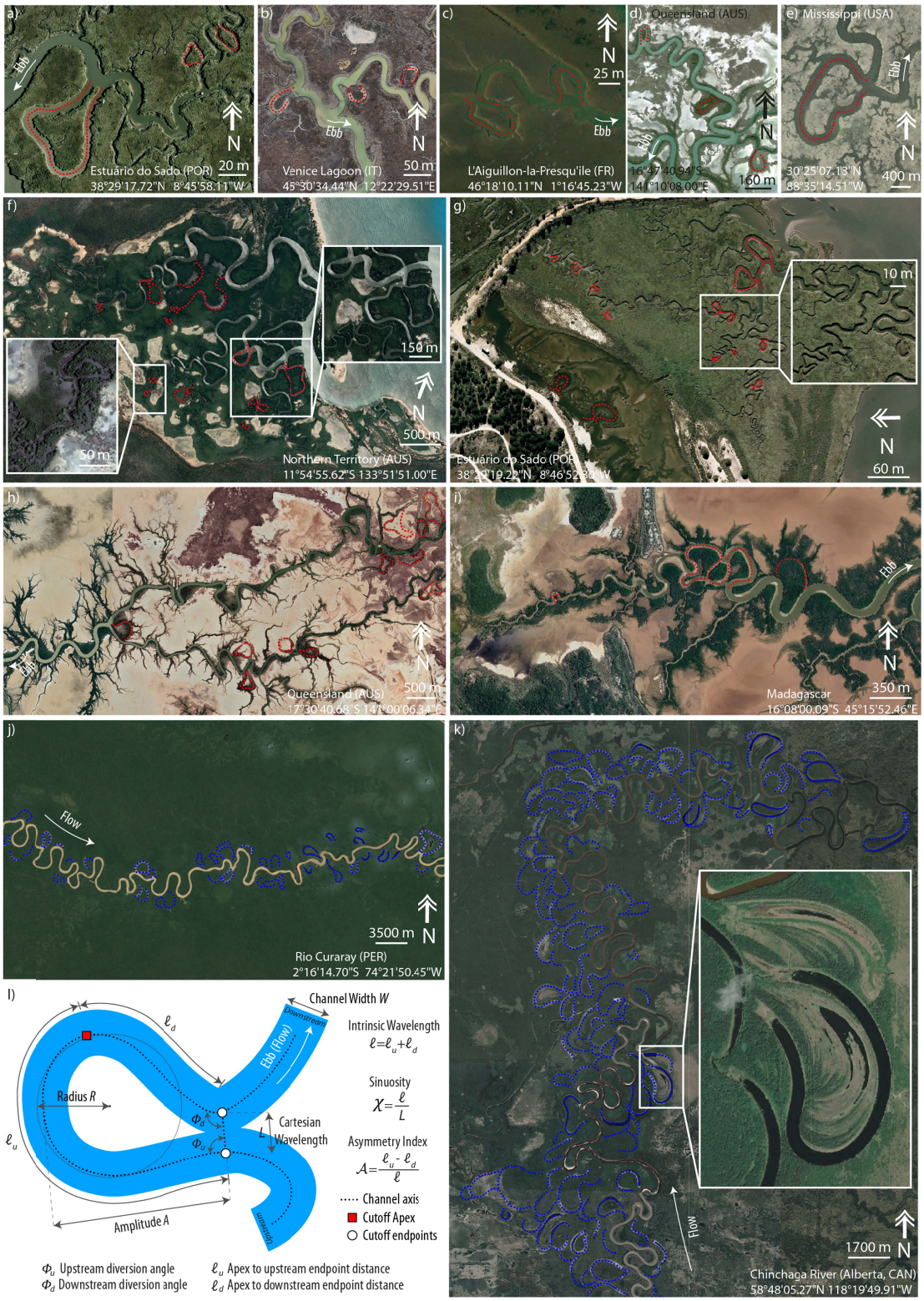

Figure 1. Meander cutoffs in tidal and fluvial landscapes. (a,b,c,d) Examples of individual tidal meander cutoffs from distinct coastal settings worldwide (image© Google: Maxar Technologies and USDA/FPAC/GEO). (f,g,h,i) Examples of tidal environments characterized by widespread meander

cutoffs (image©Google: TerraMetrics, CNES/Airbus, Maxar Technologies, Landsat/Copernicus). (j,k) Examples of river floodplains littered by oxbow lakes and cutoff traces (image©Google: Maxar Technologies). Geographic coordinates are reported in each panel. Dotted red and blue lines highlight discernable traces of meander cutoffs in tidal and fluvial landscapes, respectively. l) Sketch illustrating the main morphometric features of meander cutoffs analyzed in this study.

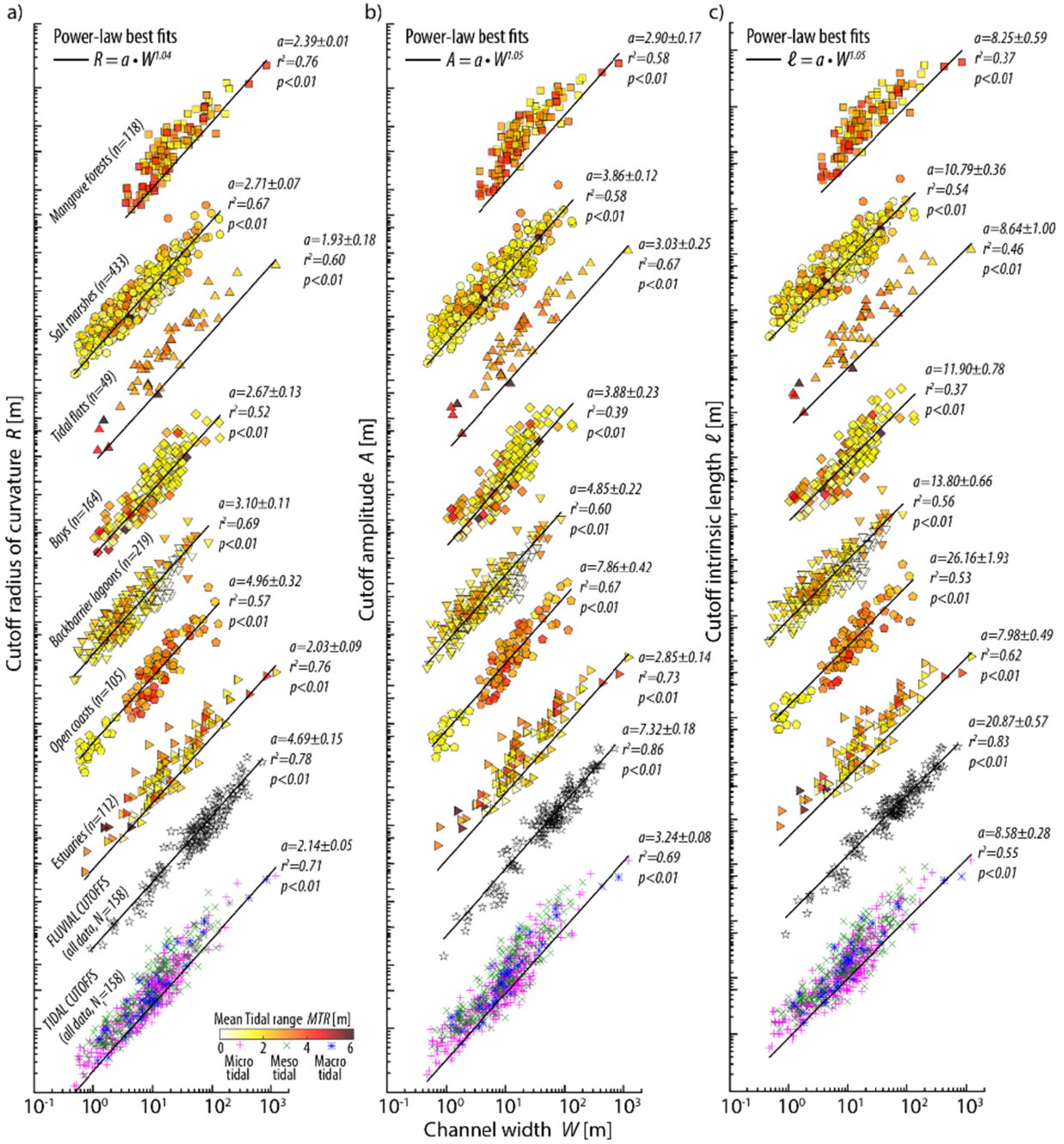

Figure 2. Cutoff morphometrics. Cutoff radius of curvature (*R*), Amplitude (***A***), and intrinsic length (***ℓ***) are plotted against channel width (*W*) both separately for all tidal and fluvial cutoffs on record and for different tidal-cutoff ensembles based on geomorphological settings and vegetation cover color-coded based on tidal ranges. Note the arbitrary vertical offset. Continuous black lines represent best-fit power law regressions obtained for different data ensembles, using a common exponent derived from all data and applied to calculate scaling coefficients for each ensemble.

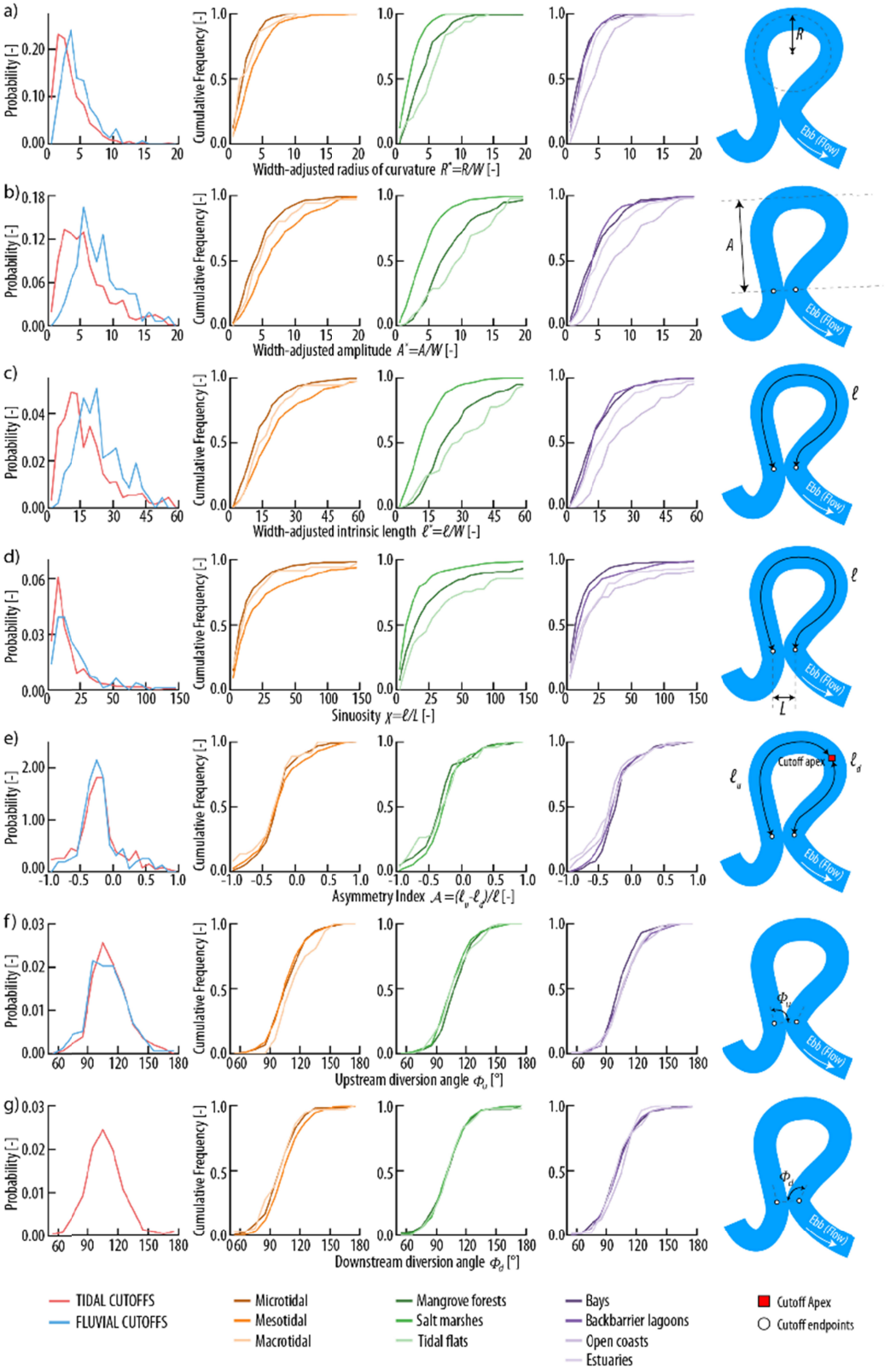

Figure 3. Dimensionless cutoff morphometrics. (a) Width-adjusted radius of curvature; (b) width-adjusted amplitude (c) width-adjusted intrinsic length; (d) sinuosity (χ); (e) asymmetry index ($\mathcal{A}$); (f,g)

595 upstream and downstream flow-diversion angles ($\boldsymbol{\Phi_u}$ and $\boldsymbol{\Phi_d}$). Panels in the first column show empirical
596 probability distributions for tidal (red) and fluvial (blue) cutoffs. Panels in the other columns report
597 empirical cumulative frequency distributions for tidal cutoffs subdivided based on tidal range, vegetation
598 cover, and geomorphological setting. The fifth column contains sketch-up views for each investigated
599 morphometric.

600

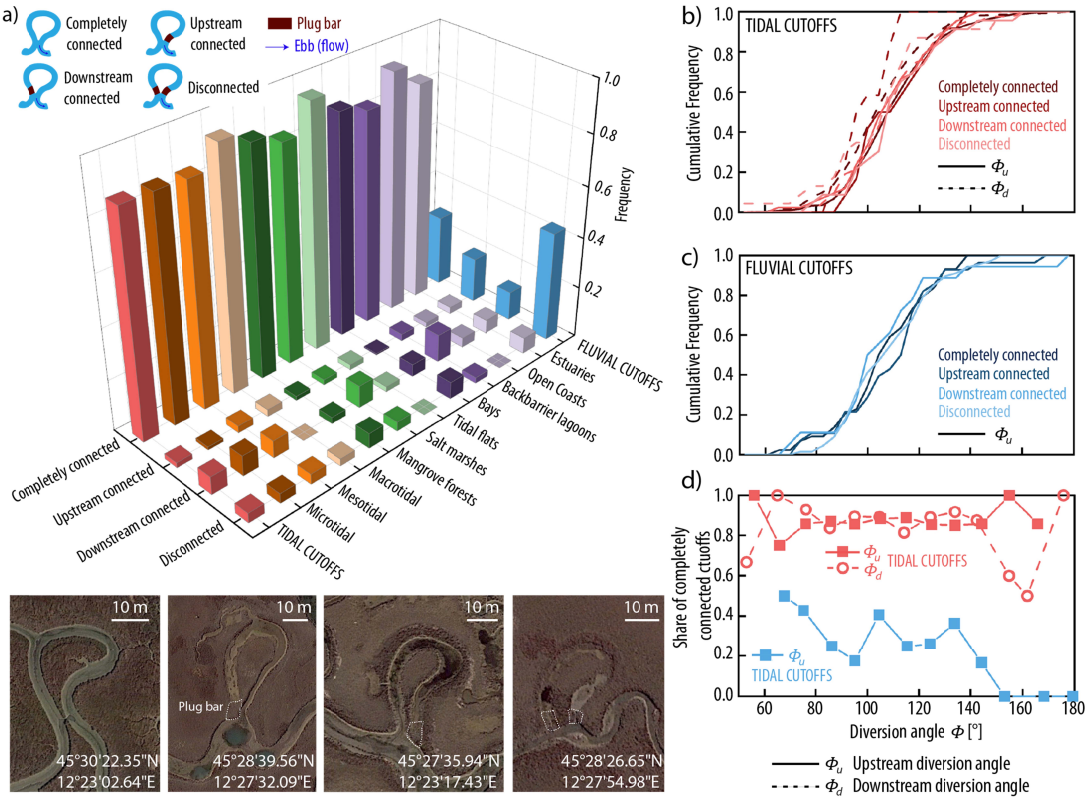

Figure 4. Cutoff connectivity. (a) Barplot showing the relative frequency of different connection types between cutoffs and parent channels, differentiating tidal (red) and fluvial (blue) cutoffs, and further segmenting tidal cutoff ensembles based on tidal range (orange), vegetation cover (green), and geomorphological settings (purple). (b,c) Frequency distributions of flow-diversion angles (Φ) for tidal and fluvial cutoffs. Different colors denote different connectivity with the parent channel. Solid and dashed lines denote upstream and downstream diversion angles, respectively. (d) Share of completely connected tidal (red) and fluvial (blue) cutoffs across uniform 10° diversion-angle intervals. Solid squares and empty dots denote upstream and downstream diversion angles, respectively. (e) Tidal cutoffs found in the microtidal lagoon of Venice (Italy) characterized by different connectivity.